Aerodynamic Design Methodology for Blended Wing Body Transport

LI Peifeng[a], ZHANG Binqian[a,*], CHEN Yingchun[a,b], YUAN Changsheng[a], LIN Yu[a]

[a]College of Aeronautics, Northwestern Polytechnical University, Xi'an 710072, China

[b]Shanghai Aircraft Design and Research Institute, Commercial Aircraft Corporation of China，Ltd. , Shanghai 200232, China

Abstract

This paper puts forward a design idea for blended wing body (BWB). The idea is described as that cruise point, maximum lift to drag point and pitch trim point are in the same flight attitude. According to this design idea, design objectives and constraints are defined. By applying low and high fidelity aerodynamic analysis tools, BWB aerodynamic design methodology is established by the combination of optimization design and inverse design methods. High lift to drag ratio, pitch trim and acceptable buffet margin can be achieved by this design methodology. For 300-passenger BWB configuration based on static stability design, as compared with initial configuration, the maximum lift to drag ratio and pitch trim are achieved at cruise condition, zero lift pitching moment is positive, and buffet characteristics is well. Fuel burn of 300-passenger BWB configuration is also significantly reduced as compared with conventional civil transports. Because aerodynamic design is carried out under the constraints of BWB design requirements, the design configuration fulfills the demands for interior layout and provides a solid foundation for continuous work.

Keywords: blended wing body; aerodynamic configurations; computational fluid dynamics; optimization design; inverse design

1. Introduction

With the increasing environment requirements of reductions in fuel burn, noise and NO_x emissions for the future civil transport [1], the current generation civil transports cannot fulfill these requirements. Blended wing body (BWB) configuration is gradually accepted by the aviation industry for its particular advantages, and a wide variety of investigations have been carried out at NASA [2-3], Boeing [4-7], ONERA [8] and DLR [9] for many years. In China, Northwestern Polytechnical University collaborates with Commercial Aircraft Corporation of China, Ltd. (COMAC) on 150-passenger BWB configuration design, and it may be the smallest BWB transport among current researches. As compared with the conventional civil transports, BWB configuration has more excellent aerodynamic characteristics, lower fuel burn and lower emissions because of highly integrating wing and fuselage which can reduce wetted area and weight significantly. At the same time, mounting the engines on the upper surface of BWB trailing edge, which is able to shield the forward-radiated fan noise and avoid engine exhaust noise reflecting off the lower surface of BWB, can get greater efficiency in reducing noise level [4,10-11].

The current BWB investigations mainly focus on conceptual design which is operated under the multidisciplinary design optimization (MDO) environment. The most representative researches are as follows: Massachusetts Institute of Technology and Cambridge University use a quasi-3D airframe design methodology for Silent Aircraft eXperiment (SAX) design [12-14]; Boeing company utilizes wing multidisciplinary optimization design (WingMOD) code to design BWB aircraft at high subsonic speed [4-7]. However, these design methods usually have a lot of design variables.

Aerodynamic analysis, at the conceptual design stage, always uses empirical equations and low fidelity analysis tools which may lack accurate prediction of aerodynamic force and the detail of flow phenomena. So it is greatly necessary to develop BWB aerodynamic design methodology based on high fidelity aerodynamic analysis tools.

BWB design lags behind the conventional civil transport in using the CFD-driven optimization and inverse design. The reasons why these methods are still not quickly applied lie largely in the following aspects. First, BWB pursuits high cruise efficiency. At the same time, it must satisfy a unique set of design requirements such as volume, trim, cruise deck angle and control, etc [4]. As a result, more geometric and aerodynamic constraints should be considered. Second, it is difficult to get the optimal result with the large design spaces and a lot of non-linear constraints. Third, using high fidelity aerodynamic analysis tools in the optimization design leads to huge computational costs, and thus becomes a major obstacle to the incorporation of CFD-driven optimization into the BWB design [15]. Last, it is difficult to obtain the target pressure distribution for inverse design. As mentioned above, more design requirements must be considered. The conversion of design requirements into pressure distribution is difficult, and moreover, BWB design is a complex 3D problem [15]. Maybe a skillful designer can come up with successful pressure distribution. Thus, defining the proper target pressure distribution according to design requirements and flow characteristics of BWB is a key point [16].

Based on the current investigations, the paper puts forward a design idea which is described as cruise point, maximum lift to drag point and pitch trim point are in the same flight attitude, and develops a corresponding design methodology. By using the low and high fidelity aerodynamic analysis tools，the BWB aerodynamic design methodology that satisfies the design requirements is established with the combination of optimization and inverse design methods.

2. Design Methodology

The core of the present aerodynamic design methodology can be generalized as follows. Planform optimization design is a dominant step, and then wing section inverse design is a supplementary step. The design process, as shown in Fig. 1, can be accomplished by MATLAB software.

2.1. Geometry definition

In the early work, we have designed several airfoils which are placed in the center body, blending area and outer wing according to the BWB design requirements. Once the planform design variables are defined, the 3D geometry of BWB configuration can be constructed with the airfoils and geometric constraints. The detail will be shown in the following section.
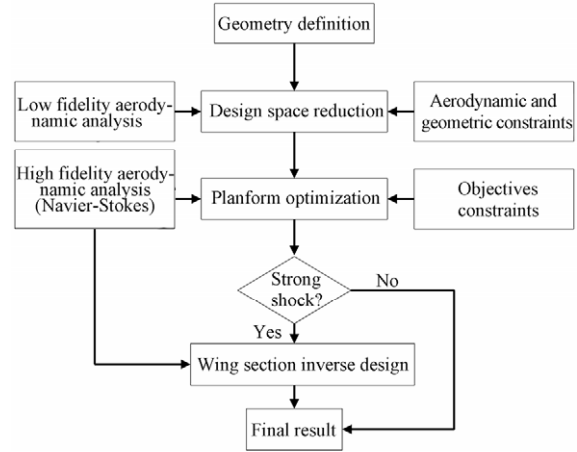

Fig. 1   Flowchart of design methodology.

2.2. Design space

1) Principle

Based on the selected design variables, a large number of sample points are generated in the initial large design spaces according to a design of experiment (DOE) technique named Latin hypercube sampling (LHS) [17], which fills the design spaces with sufficient sample points and ensures proper spatial distribution of these sample points, thus having the advantage of better reflection on design spaces.

In order to get the reasonable design spaces for the high fidelity CFD-driven optimization, we apply low fidelity aerodynamic analysis tools to eliminate useless sample points from the initial large design spaces by aerodynamic and geometric constraints. For example, the sample points whose wing sweep are low may lead to strong shock wave at transonic speed, and the sample points with forward swept wing do not satisfy the geometric constraints. These sample points are unreasonable from the views of aerodynamic and geometric requirements, and should be filtered out.

2) Low fidelity aerodynamic analysis module

According to the researches of Hileman, et al. [12-14] and Ko [18], low fidelity aerodynamic analysis module, with high efficiency but adequate accuracy, is developed in this paper. Figure 2 shows the schematic diagram of low fidelity aerodynamics analysis module.
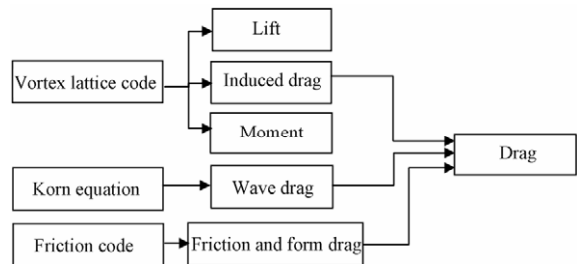

Fig. 2   Schematic diagram of low fidelity aerodynamic analysis module.

As shown in Fig. 2, low fidelity aerodynamic analysis module can be broken up into three aspects: a) A vortex lattice code is used to calculate lift, induced

drag and moment coefficients; b) Friction code is used to calculate the friction and form drag coefficients with a strip method described in Ref. [18]; c) Korn equation is an easy and effective way to calculate the wave drag. The detail of this method, which can be found in Ref. [18], is described as an empirical equation. Maybe low fidelity aerodynamic analysis will not predict accurate aerodynamic force, but it still has the ability to capture the global trends of the variation in aerodynamic characteristics. Validation of this aerodynamic analysis module with 150-passenger BWB configuration, as shown in Fig. 3, demonstrates that low fidelity results match well with Navier-Stokes results. In Fig. 3, C_L is the lift coefficient, C_D the drag coefficient, K the lift to drag ratio, α the angle of attack. Boeing company's WingMOD code and SAX's quasi-3D airframe design methodology also demonstrate the design methodology based on the fact that a vortex lattice method is feasible.
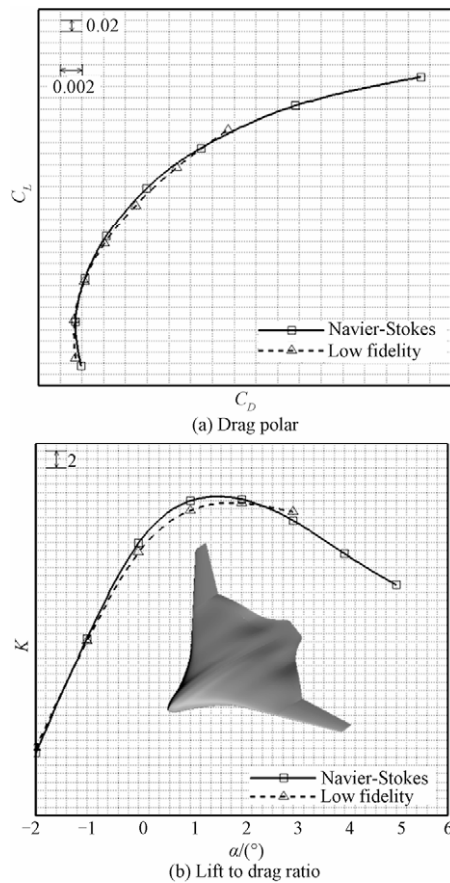

Fig. 3　Validation of aerodynamic analysis module with 150-passenger BWB configuration.

2.3. CFD-driven optimization

1) Optimization method

This paper uses the combination of response surface methodology (RSM) and genetic algorithm (GA) to optimize the planform of BWB. RSM is widely used due to its relatively low computational costs and easy elimination of numerical noise, thus improving the optimization efficiency [19-20]. The optimization process can be presented as follows.

First, LHS is used to generate sample points in the filtered design spaces which are described in Section 2.2. Second, using Navier-Strokes solver to evaluate the response values of these sample points, and then a second-order polynomial response surface model, as shown in Eq. (1), is generated, where $X_i^{(q)}$ and $X_j^{(q)}$ are design variables, b_0, b_i and b_{ij} are regression coefficients, and $Y^{(q)}$ is response value. For n design variables, there are $(n+1)(n+2)/2$ unknown regression coefficients which can be solved by the method of least squares. The coefficients of multiple determination R^2 and R_a^2 (R-square adjusted) are used to measure the accuracy of response surface model. R^2 and R_a^2 range from 0 to 1. More details can be found in Refs. [19]-[20]. Response surface model can be considered to be reliable if both R^2 and R_a^2 are close to 1. Typical number of sample points n_s is 1.5-3 times of the regression coefficients.

$$\begin{cases} Y^{(q)} = b_0 + \sum_{i=1}^{n} b_i X_i^{(q)} + \sum_{i=1}^{n}\sum_{j=1}^{n} b_{ij} X_i^{(q)} X_j^{(q)} \\ q = 1, 2, \cdots, n_s \end{cases} \quad (1)$$

Third, based on defined objectives and constraints, GA is used to optimize the design problem.

2) CFD method

Reynolds-averaged Navier-Stokes solver is used for CFD-driven optimization，Eq. (2) gives the integral form of the conservation equations:

$$\frac{\partial}{\partial t}\iiint \boldsymbol{Q} \mathrm{d}v + \iint \boldsymbol{f} \cdot \boldsymbol{n} \mathrm{d}s = 0 \quad (2)$$

where v is the cell volume, s the cell surface, $\boldsymbol{n}$ the unit outward normal vector, $\boldsymbol{Q}$ the vector of conserved variables, and $\boldsymbol{f}$ the net flux through a surface s. Finite volume approach is used to solve the equations in a conservative form. An upwind-biased, Roe's flux difference splitting (FDS) scheme is used to solve the inviscid terms. A second-order central difference method is used to discretize the viscous terms. An implicit method is used for time marching. Spalart-Allmaras one-equation model is used for full turbulence computation. Multi-grid algorithm is used to accelerate convergence to steady state. In the current work, we use ONERA M6 wing to validate the accuracy of the flow solver at Mach number $Ma=0.839\,9$, $\alpha=3.06°$ and Reynolds number $Re=11.72\times10^6$. A C-H type grid, as shown in Fig. 4, consisting of $177\times129\times65$ grid points is used. The surface pressure distributions, as shown in Fig. 5, are captured well by computation when compared with the experimental results. The difference between computation and experiment at $z/B=0.20$ (z represents spanwise position, and B half-span) comes from the wall interference of wind tunnel test, which has not been considered in computation.
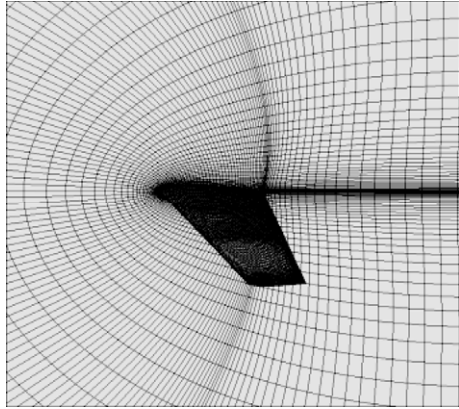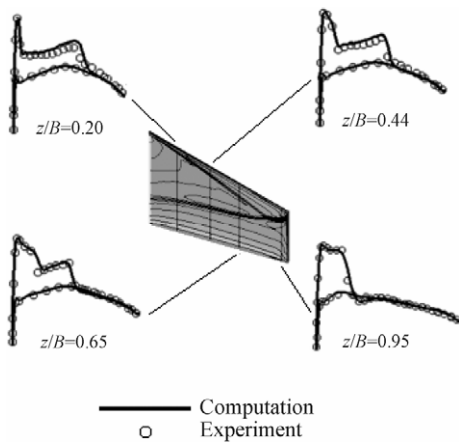
Fig. 4   Grid for ONERA M6 wing.

Fig. 5   Comparison of surface pressure distributions.

2.4. CFD-driven inverse design

Planform optimization is the core of BWB design methodology. Reasonable matching of planform variables can improve aerodynamic characteristics significantly, but it has a limit on controlling the shock wave which can be weakened by modifying the profile of wing section. As a matter of fact, transonic flow is very sensitive to the slight disturbance of the airfoil profile. Unreasonable design variables and spaces may lead to an imperfect result if the optimization design is used. Moreover, the computational costs are huge. CFD-driven inverse design presents greater efficiency in weakening the shock wave and improving the aerodynamic characteristics of BWB. In this paper, pressure distribution in shock region is modified by designer, and then the airfoil is redesigned with less computational costs.

In the present design methodology, direct iterative surface curvature (DISC) method [21-22] coupling with Navier-Stokes solver is used for inverse design. The detail of DISC method can be found in Ref. [21]. As a rule，different algorithms are adopted in different regions. In subsonic regions, the relationship between the change in surface pressure coefficient and the change in surface curvature can be written as

$$\Delta C = \Delta C_p A (1 + C^2)^D \qquad (3)$$

where $A = 1$ and -1 represent the upper and lower surfaces of the airfoil, C is the surface curvature, ΔC the change in surface curvature, ΔC_p the change in surface pressure coefficient, and D a constant ranging from 0 and 0.5. The change in surface curvature is then converted to the change in second derivative of coordinate y:

$$\Delta y'' = \Delta C [1 + (y')^2]^{1.5} \qquad (4)$$

In supersonic regions, based on supersonic thin airfoil theory, the formula of the change in second derivative of coordinate y is given as

$$\Delta y'' = k \mathrm{d}(\Delta C_p) / \mathrm{d}x \qquad (5)$$

with $k = 0.05$ for typical cases.

When $\Delta y''$ is obtained, the corresponding Δy can be calculated by integration of Eqs. (4)-(5). Navier-Stokes solver is used for flow simulation of the new airfoil which is generated by adding Δy to the initial airfoil, and then inverse design process is driven by calculating the difference between new pressure distribution and target pressure distribution. The iterative process repeats until the final pressure distribution matches well with the target pressure distribution.

3. BWB Design

The detail of the design idea is described in Section 2, and then Section 3 uses the design methodology to design 300-passenger BWB configuration. In the following research, all the aerodynamic coefficients are based on reference area and reference length which are determined by the total area of BWB.

3.1. Geometry and design variables

Planform and typical airfoils of BWB configuration are shown in Fig. 6. Nine airfoils are located in spanwise direction, where 1-4 is the center body, 4-6 is the blending area, and 6-9 is the outer wing. Coordinates of x and z represent chordwise and spanwise positions, c_r represents root chord of BWB. For the sake of simplicity, a linear interpolation of adjacent airfoils is applied to constructing the 3D geometry of BWB configuration.
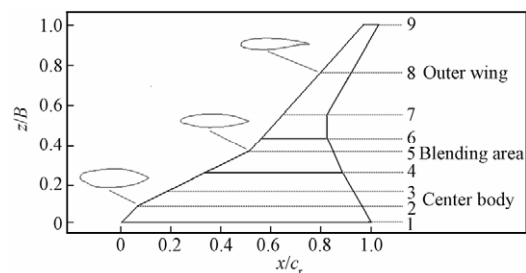
As shown in Fig. 6, 13 design variables are defined

Fig. 6   Planform and airfoils of BWB configuration.

as follows. x coordinate of leading edge: x_{L4}, x_{L5} and x_{L9}, z coordinate of leading edge: z_6 and z_7, local chord of wing section: c_5, c_6 and c_9, geometric twist angle: a_{t1}, a_{t6}, a_{t7}, a_{t8} and a_{t9}. In order to satisfy design requirements as well as simplify the research, geometric constraints, as shown in Eqs. a)-h), are given in the design process:

a) $T_i = \text{const}_i$, i=1-4.

b) $z_4 = \text{const}$.

c) $x_{Ti} = \text{const}_i$, i = 2-4.

d) $a_{ti} = a_{t1}$, i = 2-4.

e) $x_{Li} = (z_i - z_5)(x_{L9} - x_{L5})/(z_{L9} - z_{L5}) + x_{L5}$, i = 6-8

$x_{Lj} = (z_j - z_2)(x_{L4} - x_{L2})/(z_{L4} - z_{L2}) + x_{L2}$, j = 3.

f) $\Lambda_{Ti} = 0$, i=6-7.

g) c_r, x_{L2}, z_2, z_3, z_5, z_8, z_9, $a_{t5} = \text{const}$

h) $(T/c)_i = \text{const}_i$, i = 5-9.

In order to accommodate passenger cabin and cargo containers in the center body, Eq. a) gives the thickness T constraints of wing sections at the center body. During the planform optimization design process, each wing section's thickness-to-chord ratio is changed so as to satisfy the thickness constraints. Eq. b) gives the spanwise dimension constraint of passenger cabin. Eq. c) gives the constraints of x coordinate at the trailing edge x_T. With enough aft center body area, it is easy to install the engines and elevator. Eq. d) guarantees the same value of geometric twist angle at center body. Eqs. e)-g) give the geometric simplicity of BWB, and Eq. e) gives the formulas for calculating x_{L3}, x_{L6}, x_{L7}, x_{L8}, Eq. f) keeps a zero trailing edge sweepback angle Λ_T on the inner side of the outer wing ($i = 6\text{-}7$), Eq. g) keeps constant values of c_r, x_{L2}, z_2, z_3, z_5, z_8, z_9, a_{t5} during the planform optimization. Eq. h) gives the thickness-to-chord ratio T/c constraints at blending area and outer wing so that the thickness-to-chord ratios of corresponding wing sections are kept constant.

3.2. Design space reduction

According to the discussion of geometry and design variables, design space reduction which is similar to the research of high speed civil transport (HSCT) [23] design is carried out at BWB cruise condition: Ma=0.8, α=2° and H=11 km (H represents the height). Geometric twist angles are kept constant and design variables of x_{L4}, x_{L5}, x_{L9}, z_6, z_7, c_5, c_6 and c_9 are changed so as to achieve the variation of shape during the design space reduction. Figure 7 shows the comparison of design spaces, where the variation of shape cannot go beyond the boundary described by dashed line.

2 000 BWB sample points are generated by LHS in the initial design spaces which are large in dimension, and the boundary of large design spaces is shown in Fig. 7(a). Low fidelity aerodynamic analysis module is adopted to evaluate aerodynamic characteristics of these sample points. As planform modification may yield significant changes in aerodynamic performance,
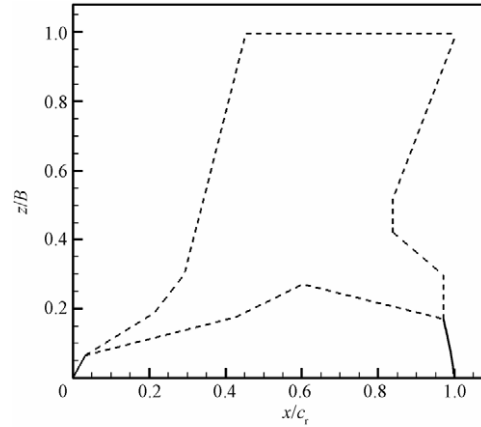
(a) Boundary of initial design spaces
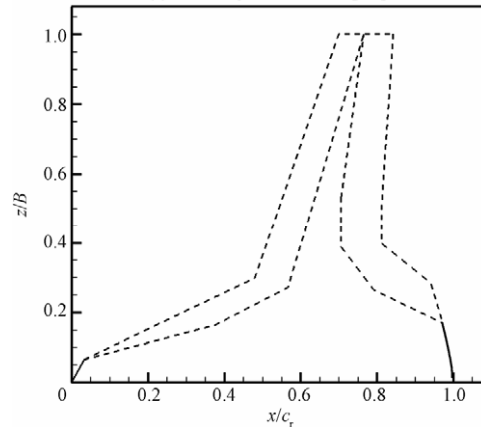
(b) Boundary of final design spaces

Fig. 7　Comparison of design spaces (dashed line stands for boundary of design spaces).

lift to drag ratio K, wave drag coefficient C_{Dw} and moment coefficient C_m of the initial configuration are set as criteria for design space reduction, and constraints of leading edge sweepback angle Λ_L are also given. The corresponding constraints (subscript "I" represents initial configuration, and "max" represents upper limit) are defined as follows:

$$\begin{cases} K \geq K_I \\ C_{Dw} \leq C_{DwI} \\ C_{m\max} \geq C_m \geq C_{mI} \\ \Lambda_{Li} > 0 \quad i = 5, 6, \cdots, 9 \end{cases} \tag{6}$$

The sample points whose aerodynamic coefficients and geometry do not fulfill the constraints will be filtered out, thus reducing the initial design spaces. The boundary of final design spaces, as shown in Fig. 7(b), is smaller in dimension than that of the initial design spaces.

3.3. Planform optimization design

Objective and constraint are defined based on design requirements. RSM combined with GA is then used to optimize the problem in the filtered design spaces which are described in Section 3.2.

1)Objective and constraint

Analyzing aerodynamic force and flow characteristics of initial BWB by Navier-Stokes solver and considering the design requirements, we put forward objectives and constraints. This design is a multipoint optimization problem and three conditions are mainly taken into consideration: cruise, negative lift and buffet margin. For the first design point, cruise condition is at $Ma=0.8$, $\alpha=2°$ and $H=11$ km. In order to gain high cruise efficiency, an objective is defined as improving lift to drag ratio K_1 (subscript "1" represents cruise condition). For a pitch trim state at cruise condition, it is generally believed that $C_{m1}=0$ is the perfect condition, and moreover, a lift constraint is also given. For the second design point, negative lift condition is at $Ma=0.8$, $\alpha=-2°$ and $H=11$ km. Zero lift pitching moment C_{m0} is obtained by a linear interpolation of C_{m1} and C_{m2} (subscript "2" represents negative lift condition). For static stability and pitch trim considerations, C_{m0} must be greater than zero, so $\partial C_m/\partial C_L<0$. For the third design point, buffet margin condition is set at $Ma=0.8$, $C_{L3}=1.5C_{L1}$ and $H=11$ km. Buffet onset, as defined by the break in the pitching moment curve, does not occur until well beyond 1.5 times of cruise C_L, and the pitch break is mild, indicating that post-buffet pitch-up characteristics will not be severe [7]. The first and second design points are optimized in advance so as to reduce computational costs. The optimal result is considered to be feasible if buffet margin satisfies the design requirements, otherwise a three-point optimization design which includes third design point will be carried out.

The corresponding objectives and constraints for the two-point optimization design are defined as follows:

$$\begin{cases} \text{Objective: max } K_1 \\ \text{Constraint: } C_{L1} \geq C_{L11}, \ C_{m1} \cong 0, \ C_{m0} > 0 \end{cases} \quad (7)$$

2) Optimization

For a two-point optimization design problem, LHS is used to generate 270 sample points in the filtered design spaces based on 13 design variables. Aerodynamic characteristics of these sample points are evaluated with 270×2 calls for Navier-Stokes solver. Considering a large number of computational tasks, distributed parallel computation is applied to improving computational efficiency. With the response values of these sample points, response surface models are constructed for the objectives and constraints. GA is then applied to gaining the optimal result. For this case, parameters of GA are shown as follows. The population size is 100, crossover probability 0.80, and mutation probability 0.02. Table 1 shows the fitting accuracy of response surface models. Both R^2 and R_a^2 are

close to 1, which indicates a high degree of fitting accuracy.

Aerodynamic comparisons of initial configuration and optimal configuration are shown in Fig. 8. With less design variables, it is easy to satisfy design objectives and constraints by planform optimization. At cruise condition, as shown in Figs. 8(b)-8(c), improvement in lift to drag ration is 2 and a pitch trim state is achieved. Positive zero lift pitching moment is obtained because of static stability design and positive C_{m2}. The lift coefficient of the break in pitching moment is two times larger than cruise C_L, which demonstrates that the optimal configuration has better buffet characteristics.
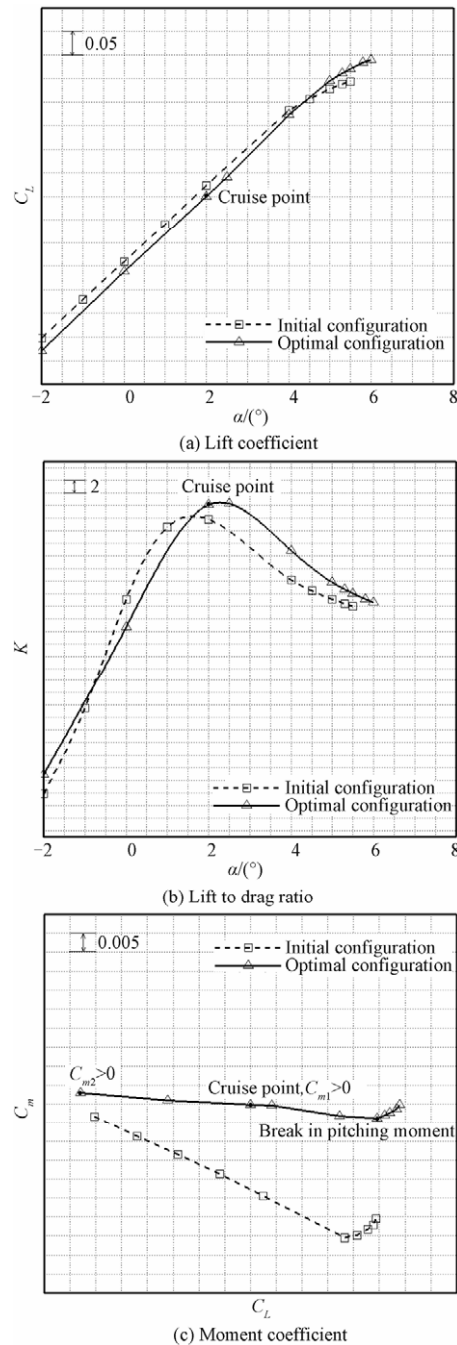

(a) Lift coefficient

(b) Lift to drag ratio

(c) Moment coefficient

Fig. 8   Comparison of aerodynamic characteristics.

Table 1   Fitting accuracy of response surface models

RSM	R^2	R_a^2
K_1	0.998 7	0.998 5
C_{L1}	0.999 1	0.998 9
C_{m1}	0.999 8	0.999 5
C_{m0}	0.998 2	0.997 9

Figure 9 shows the surface pressure coefficient C_p distributions (cruise condition) and planform comparisons of initial configuration and optimal configuration. Planform optimization, on the premise of design requirements, decreases the area at blending section which is considered as low aerodynamic efficiency and increases the area at outer wing. At the same time, variation in geometric twist angle of optimal configuration, as shown in Fig. 10, indicates that the values of geometric twist angle at out wing (from 0.37 to 1.0) are decreased when compared with initial configuration. The decreased geometric twist angles have the function of reducing local angles of attack, which can decrease loading and weaken shock strength at outer wing. These two factors are the main reasons for improvement of aerodynamic characteristics. However, local shock wave, as shown in Fig. 9, is still existent. From the surface pressure coefficient distribution we can conclude that the shock strength is weak, but it still influences the flow characteristics. Thus, in order to get more improvements, it is necessary to eliminate shock wave at outer wing.
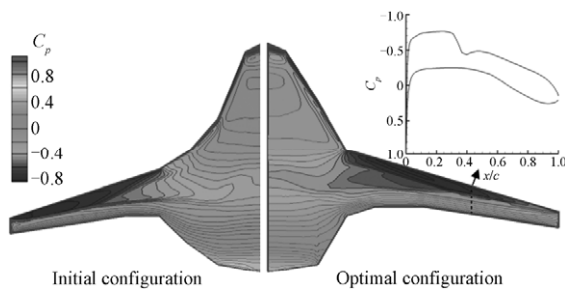

Fig. 9   Comparison of surface pressure coefficient distributions (cruise condition) and planform.
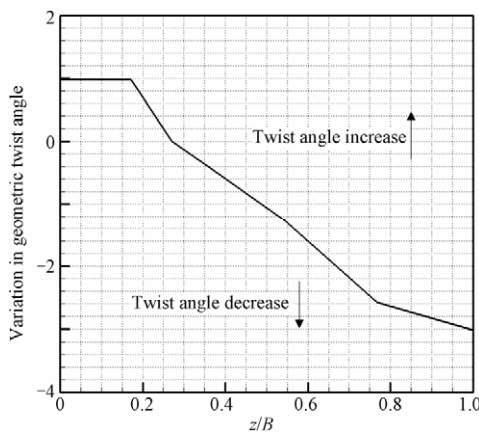

Fig. 10   Variation in geometric twist angle of optimal configuration (optimal geometric twist angle minus initial geometric twist angle).

3.4. Inverse design

Planform optimization, as described in Section 3.3, improves aerodynamic characteristics significantly, but it has a limit on controlling the local shock wave. Shock free wing can be achieved by modifying the profile of wing section. In this section, according to the

flow characteristics of optimal configuration, pressure distribution in shock wave region is modified by designer and then a 3D inverse design method is used to eliminate the shock wave.

Optimal configuration is taken as initial configuration (in Section 3.4, initial configuration represents optimal configuration and design configuration represents inverse design configuration) and 70% semi-span is chosen for inverse design. As for target pressure coefficient distribution, two aspects are taken into consideration. First, shape variation of wing section should be small, otherwise a large shape variation may lead to a bad change in aerodynamic characteristics at transonic speed. Thus, reshaping of the pressure coefficient distribution is just limited in shock region of initial wing section. Second, in order to eliminate shock wave, a slowly increase of pressure which is considered as an isentropic compression state should be used instead of pressure jump in initial shock wave region. Based on these two aspects, target pressure distribution is obtained. Figure 11(a) shows target pressure distribution which seems more reasonable. DISC method coupling with Navier-Stokes solver is applied to redesigning the wing section. After 15 design cycles, the final design pressure coefficient distribution, as shown in Fig. 11(a), matches well with target pressure coefficient distribution. The profile of design wing section, as shown in Fig. 11(b), shows a little difference when compared with initial wing section. A "bulge" that leads to a slight increase in thickness to chord ratio is found on the upper surface of the design wing section, and its function is similar to the shock control bump which can create a sufficient isentropic compression process.

(a) Surface pressure coefficients distribution
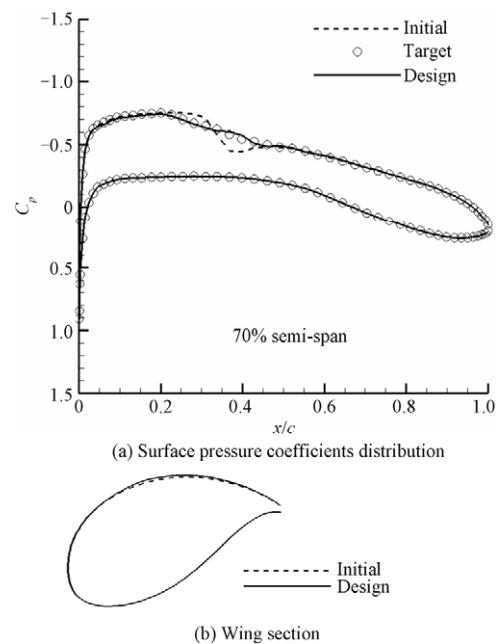

(b) Wing section

Fig. 11   Design result at 70% semi-span.

Figure 12 shows the comparison of surface pressure coefficients distribution at outer wing. Shock wave is almost eliminated by inverse design, and the design

configuration demonstrates an improvement to the initial configuration in flow characteristics. However, initial shock wave is weak as discussed in Section 3.3 and increment in thickness of the wing section may result in an additional drag increment. Figure 13 shows the comparion of lift coefficient, lift to drag ration and moment coefficient. The improvements in aerodynamic characteristics are unobvious when compared with the initial configuration.

As for inverse design configuration, Fig. 14 shows the comparison of low fidelity result and Navier-Stokes result. The maximum discrepancy of lift to drag ratio is about 2 when compared with Navier-Stokes result.
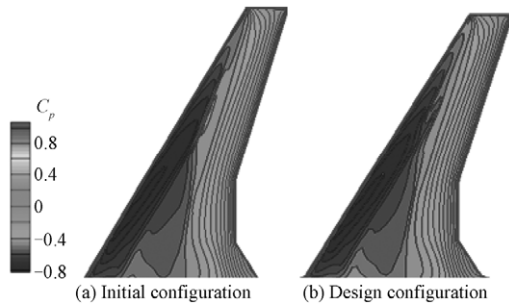

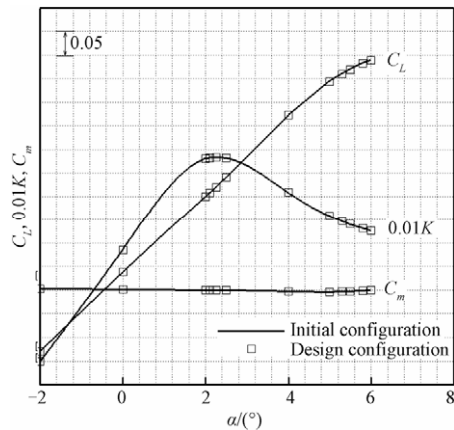Fig. 12   Comparison of surface pressure coefficient distributions at outer wing.

Fig. 13   Comparion of lift coefficient, lift to drag ration and moment coefficient.
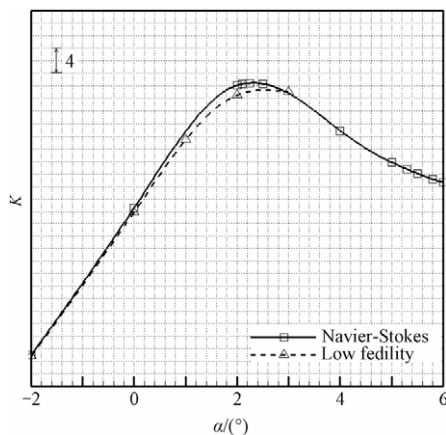

Fig. 14   Comparison of low fidelity result and Navier-Stokes result.

This is an accepted result when considering the precision and computational costs of the low fidelity method.

3.5. Result discussion

Aerodynamic design methodology, with the combination of design space reduction, optimization and inverse design, is used to gain the final BWB configuration, namely the inverse design configuration. As shown in Fig. 8 and Fig. 13, the final configuration satisfies the design requirements when compared with initial configuration. Based on static stability design, high lift to drag ratio and pitch trim are achieved at cruise condition, and buffet characteristics are also satisfied with the design requirements. Figure 15 shows the interior layout of BWB. As mentioned in Section 3.1, we consider thickness distribution (T_1-T_4) and spanwise dimension constraints (z_4) at center body along all the aerodynamic design process. Moreover, the mid-portion of center body airfoil, as shown in Fig. 6 and Fig. 15, is "flat" enough, which can provide enough space for loading. Therefore, passenger cabin, galley, lavatory, aisle areas, cargo containers and undercarriage are easily accommodated in the center body.
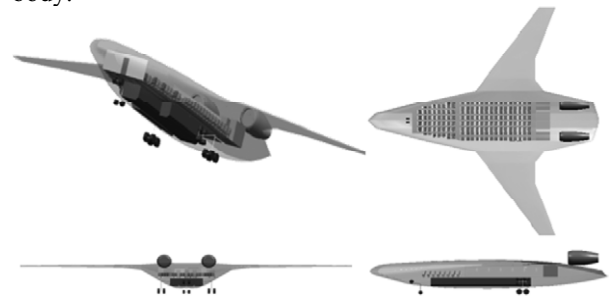

Fig. 15   Interior layout of BWB.

Fuel efficiency is a key factor to evaluate the performance of a civil transport. As shown in Table 2, fuel burn of the 300-passenger BWB with maximum takeoff weight of 190 000 kg and 13 000 km range is calculated and compared to the data of conventional civil transports. A 13% to 37% fuel burn reduction is obtained when compared to B787-3, B747-4 and A330-3, which demonstrates a better performance of BWB. As mentioned in Ref. [24], the low fuel burn of BWB comes from the high aerodynamic efficiency of the configuration and the improvement of engine efficiency.

Table 2   Comparison of fuel burn (per passenger per 100 km)

Aircraft	Fuel burn/L
B787-3	2.48
B747-4	3.39
A330-3	3.20
300-passenger BWB	2.15

4. Conclusions

The paper is aimed at developing an aerodynamic design methodology for BWB configuration, and using

this design methodology to design 300-passenger BWB configuration. Conclusions can be concluded as follows:

A design idea, which is described as cruise point, maximum lift to drag point and pitch trim point are in the same flight attitude, is put forward.

According to design requirements, using low and high fidelity aerodynamic analysis tools, BWB design methodology is established with the combination of optimization and inverse design methods.

Planform optimization is the core of the design methodology. Reasonable matching of planform variables can directly improve the aerodynamic characteristics, but it cannot control the local shock wave.

Inverse design is a good supplement to the planform optimization. By changing the pressure distribution in shock wave region, DISC method coupling with Navier-Stokes solver is used to redesign the wing section and eliminate shock wave with less computational costs.

300-passenger BWB configuration has been investigated. As compared with initial BWB configuration, design BWB configuration achieves high lift to drag ratio (improvement is 2) and pitch trim at cruise condition, fulfills positive zero lift pitching moment and static stability design requirements, and has better buffet characteristics. Moreover, interior layout is easy to achieve, and fuel burn is significantly reduced.

As the current research mainly focuses on aerodynamic characteristics at cruise speed, researches on engine effect, takeoff and landing performance will be carried out in the continuous work.

References

[1] Nickol C L, McCullers L A. Hybrid wing body configuration system studies. AIAA-2009-931, 2009.

[2] Chambers J R. Innovation in flight: research of the NASA Langley Research Center on revolutionary advanced concepts for aeronautics. NASA SP-2005-4539, 2005.

[3] Re R J. Longitudinal aerodynamic characteristics and wing pressure distributions of a blended-wing-body configuration at low and high Reynolds number. NASA/TM-2005-213754, 2005.

[4] Liebeck R H. Design of the blended wing body subsonic transport. Journal of Aircraft 2004; 41(1):10-25.

[5] Roman D, Allen J B, Liebeck R H. Aerodynamic design challenges of the blended-wing-body subsonic transport. AIAA-2000-4335, 2000.

[6] Gilmore R, Wakayama S, Roman D. Optimization of high-subsonic blended-wing-body configurations. AIAA-2002-5666, 2002.

[7] Roman D, Gilmore R, Wakayama S. Aerodynamics of high subsonic blended-wing-body configurations. AIAA-2003-554, 2003.

[8] Mialon B, Fol T, Bonnaud C. Aerodynamic optimization of subsonic flying wing configurations. AIAA-2002-2931, 2002.

[9] Mialon B, Hepperle M. Flying wing aerodynamics studied at ONERA and DLR.<http://www.onera.fr/daap/ailes-volantes/flying-wing-aerodynamics-Onera-D LR.pdf>. 2005.

[10] Carter M B, Vicroy D D, Patel D. Blended-wing-body transonic aerodynamics: summary of ground tests and sample results. AIAA-2009-935, 2009.

[11] Clark L R, Gerhold C H. Inlet noise reduction by shielding for the blended-wing-body airplane. AIAA-1999-1937, 1999.

[12] Hileman J I, Spakovszky Z S, Drela M, et al. Airframe design for silent fuel-efficient aircraft. Journal of Aircraft 2010; 47(3): 956-969.

[13] Hileman J I, Spakovszky Z S, Drela M, et al. Aerodynamic and aeroacoustic three-dimensional design for a "silent" aircraft. AIAA-2006-241, 2006.

[14] Hileman J I, Spakovszky Z S, Drela M, et al. Airframe design for "silent" aircraft. AIAA-2007-453, 2007.

[15] Peigin S, Epstein B. Computational fluid dynamics driven optimization of blended wing body aircraft. AIAA Journal 2006; 44(11): 2736-2745.

[16] Pambagjo T E, Nakahashi K, Obayashi S, et al. Aerodynamic design of a medium size blended wing body airplane. AIAA-2001-0129, 2001.

[17] Giunta A A, Wojtkiewicz S F, Eldred M S. Overview of modern design of experiments methods for computational simulations. AIAA-2003-649, 2003.

[18] Ko Y Y A. The multidisciplinary design optimization of a distributed propulsion blended wing body aircraft. PhD thesis, Virginia Polytechnic Institute and State University, 2003.

[19] Ahn J, Yee K, Lee D H. Two-point design optimization of transonic airfoil using response surface methodology. AIAA-1999-0403, 1999.

[20] Madsen J I, Shyy W, Haftka R T. Response surface techniques for diffuser shape optimization. AIAA Journal 2000; 38(9):1512-1518.

[21] Campbell R L，Smith L A. A hybrid algorithm for transonic airfoil and wing design. AIAA-1987-2552, 1987.

[22] Yu N J，Campbell R L. Transonic airfoil and wing design using Navier-Strokes codes. AIAA-1992-2651, 1992.

[23] Giunta A A, Narducci R, Burgee S, et al. Variable complexity response surface aerodynamic design of an HSTC wing. AIAA-1995-1886, 1995.

[24] Diedrich A, Hileman J, Tan D, et al. Multidisciplinary design and optimization of the silent aircraft. AIAA-2006-1323, 2006.

Biographies:

LI Peifeng received B.S. and M.S. degrees from Northwestern Polytechnical University in 2005 and 2008 respectively, and now is a Ph.D. candidate there. His main research interest is aerodynamic design of aircraft.
E-mail: leeona@163.com

ZHANG Binqian is a professor and Ph.D. supervisor in Northwestern Polytechnical University. His main research interest is aerodynamic design of aircraft and flow control.
E-mail: bqzhang@nwpu.edu.cn

CHEN Yingchun is a deputy chief designer of the C919, Commercial Aircraft Corporation of China, Ltd. His main research interest is aircraft design.
E-mail: chenyingchun@comac.cc